

Nitrogen radical-triggered trifunctionalizing ipso-spirocyclization of unactivated alkenes with vinyl azides towards new spiroaminal frameworks

Zhongyu Qi

Southwest Medical University

Zhijie Zhang

Southwest Medical University

Li Yang

Southwest Medical University

Di Zhang

Southwest Medical University

Siping Wei

Southwest Medical University

Qiang Fu

Southwest Medical University

Xi Du

Southwest Medical University

Dong Yi (✉ yidong@swmu.edu.cn)

Southwest Medical University <https://orcid.org/0000-0002-8281-7860>

Article

Keywords: Radical-mediated spirocyclization, spirocyclic frameworks, alkenes

Posted Date: April 2nd, 2021

DOI: <https://doi.org/10.21203/rs.3.rs-358793/v1>

License: © ⓘ This work is licensed under a Creative Commons Attribution 4.0 International License.

[Read Full License](#)

Nitrogen radical-triggered trifunctionalizing *ipso*-spirocyclization of unactivated alkenes with vinyl azides towards new spiroaminal frameworks

Zhongyu Qi^{1‡}, Zhijie Zhang^{1‡}, Li Yang¹, Di Zhang¹, Siping Wei¹, Qiang Fu^{1*}, Xi Du^{3*} & Dong Yi^{1,2*}

¹Department of Medicinal Chemistry, School of Pharmacy, Southwest Medical University, Luzhou 646000, P. R. China

²Department of Pharmacy, Affiliated Hospital, Southwest Medical University, Luzhou 646000, P. R. China

³Department of Chemistry, School of Basic Medical Science, Southwest Medical University, Luzhou 646000, P. R. China

[‡]Z.Q. and Z.Z. contributed equally.

*Correspondence: fuqiang@swmu.edu.cn, dx.d@163.com, yidong@swmu.edu.cn

ABSTRACT: Radical-mediated spirocyclization is a powerful and efficient tool to forge complex spirocyclic frameworks. Radical-mediated non-dearomative double-cyclization of linear precursors for the concomitant construction of both rings is more challenging but highly attractive. Herein, we report the first example of non-dearomative trifunctionalizing *ipso*-spirocyclization of unactivated alkenes through photoredox-catalyzed, nitrogen radical-triggered cyclization-trapping-translocation-cyclization cascade, providing a single-step modular access to architecturally new and fascinating spiroaminal frameworks through simultaneous formation of one C–C bond and two geminal C–N bonds. The developed protocol utilizes not only internal or terminal olefinic oxime esters but also olefinic amides as nitrogen radical precursors, and features broad substrate scope, varied functional group compatibility, easy scalability, and potential for product derivatization and late-stage functionalization of biologically active molecule. Importantly, the mechanistic studies including DFT calculations indicate that such photocatalytic trifunctionalizing *ipso*-spirocyclization undergoes a radical relay cascade of intramolecular *5-exo-trig* cyclization, intermolecular radical trapping, 1,5-hydrogen

atom transfer, and sequential *5-endo-trig* cyclization, which would open up a new reaction mode of alkenes.

Spirocyclic skeletons widely occur in a plethora of naturally occurring products with broad structural diversities and diverse biological activities¹⁻⁴, and are increasingly being incorporated into drug candidates^{5, 6} (Fig. 1a). Furthermore, the inherent three-dimensional (3D) conformational constraint character of the spirocyclic skeletons enables them as one of the excellent ligand⁷⁻¹⁰ and organocatalyst^{11, 12} frameworks in the field of asymmetric catalysis. In this context, an elegant radical-mediated spirocyclization for the construction of the spirocyclic compounds, including dearomative¹³ and non-dearomative¹⁴ strategies, has been developed rapidly in the past decade. To the best of our knowledge, the existing approaches for the radical-mediated spirocyclization are solely based upon the elaboration of aromatic or aliphatic monocyclic precursors on which the second ring is newly appended, and compared with the former dearomative strategies, the latter non-dearomative strategies could provide structurally distinct spirocyclic compounds with varied functionality (Fig. 1b). However, radical-mediated non-dearomative double-cyclization of linear precursors for the concomitant construction of both rings has remained unexploited to date. Thus, the development of novel spirocyclic skeletons and evermore-effective non-dearomative spirocyclization strategies using different classes of linear starting materials are highly desirable but challenging.

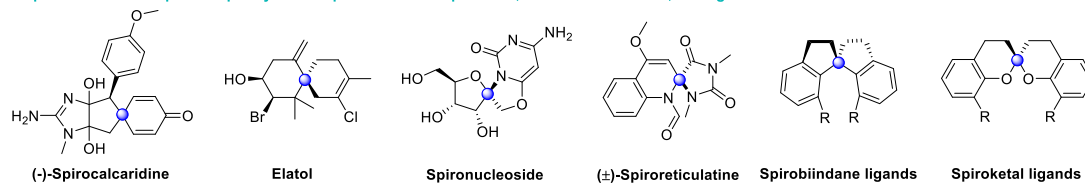
On the other hand, alkenes are energetic and versatile synthons that engage in diverse organic transformations because of their abundance and rich reactivity. In recent years, the difunctionalization of alkenes is one of the most important and valuable strategies in organic synthesis, since it allows the rapid, efficient, and synergistic incorporation of two functional groups onto one C–C double bond in an atom- and step-economic fashion for enhancing the molecular complexity and diversity. Among them, the 1,2-difunctionalization of alkenes, including intermolecular and intramolecular reactions, was extensively developed as a powerful tool for the creation of two new vicinal chemical bonds¹⁵⁻²⁰. Compared with the vigorous increasing achievements of 1,2-difunctionalization, the 1,1-difunctionalization of alkenes to

access geminal difunctionalized alkanes is still underdeveloped²¹; for example, the scope of alkene geminal diamination is limited to activated alkenes as well as ethylenediamine derivatives as nitrogen sources²²⁻²⁴. Notwithstanding the remarkable advances achieved toward the difunctionalization of alkenes, only sparsely have the more challenging trifunctionalization of alkenes been exploited, which significantly restricted their application for the assembly of diversely multifunctionalized molecules (Fig. 1c). The reason might be mainly attributed to the lack of an effective approach to realize the trifunctionalization. For the purpose of providing structurally diverse and complex functional molecule libraries derived from privileged scaffolds (particularly spirocyclic skeletons) to meet the ever-increasing demand for the development of new drugs, ligands and organocatalysts, the exploration of novel, straightforward, and efficient approaches for the trifunctionalization of alkenes is of special interest and great significance.

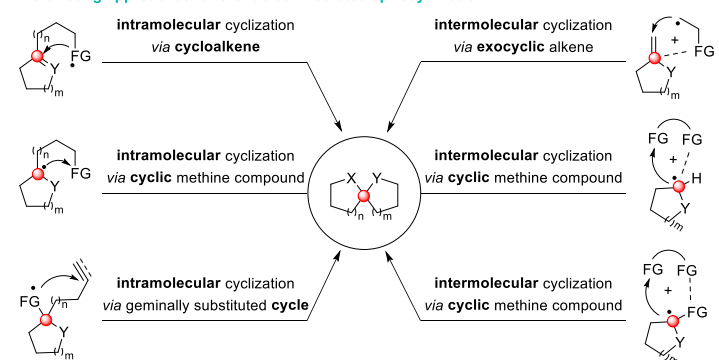
Successfully merging the difunctionalization of alkenes with the selective functionalization of C(sp³)-H bonds might be one of the reliable and effective approaches to reach the formidable trifunctionalization of alkenes. Accordingly, the strategies employed for such trifunctionalization can be largely divided into two categories: 1) very few “innate trifunctionalization”, aliphatic C(sp³)-H functionalization of the newly generated difunctionalized intermediates, such as β -keto sulfones derived from activated alkenes including vinyl azides²⁵ and styrenes²⁶, is solely based on the inherent reactivity of aliphatic C(sp³)-H bonds; 2) unexploited “guided trifunctionalization”, selective functionalization of inert aliphatic C(sp³)-H bonds in the resulting difunctionalized intermediates is guided by the external reagents or directing groups armed with functionalities, such as those that can be transformed into open-shell intermediates. In recent years, the iminyl radical-directed 1,5-hydrogen atom transfer (HAT) process provides an exceptional platform for the site-selective activation and functionalization of inert C(sp³)-H bonds²⁷⁻³⁰. Meanwhile, vinyl azides have emerged as an attractive iminyl radical source generated through an intermolecular radical addition followed by the extrusion of N₂. Up to now, several elegant examples, wherein the iminyl radicals derived from vinyl azides could trigger aliphatic C(sp³)-H functionalization involving 1,5-HAT process, have been reported by

Nevado³¹, Guo³², Bolm³³, and Liu group³⁴. Inspired by elegant work on the rich reactivities of nitrogen radical precursors³⁵⁻⁴⁰, we envisioned whether the tandem radical relay strategy of the initial radical difunctionalization of alkenes and follow-up C(sp³)-H functionalization involving iminyl radical-directed 1,5-HAT process could be applicable to the guided trifunctionalization of unactivated alkenes. Herein, we report for the first example of non-dearomative trifunctionalizing *ipso*-spirocyclization of unactivated alkenes with vinyl azides through photoredox-catalyzed, nitrogen radical-triggered cyclization-trapping-translocation-cyclization (CTTC) cascade (Fig. 1d). More importantly, one C-C bond and two geminal C-N bonds could be synergistically constructed across double bonds under this photocatalytic system to enable a straightforward single-step modular synthesis of architecturally new and intriguing spiroaminals including spirobi[pyrrolines] and spiropyrroline lactams.

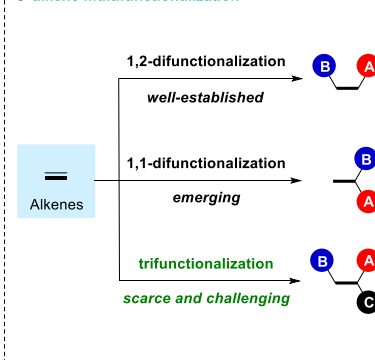
a Representative examples of spirocyclic compounds: natural products, bioactive molecules, and ligands



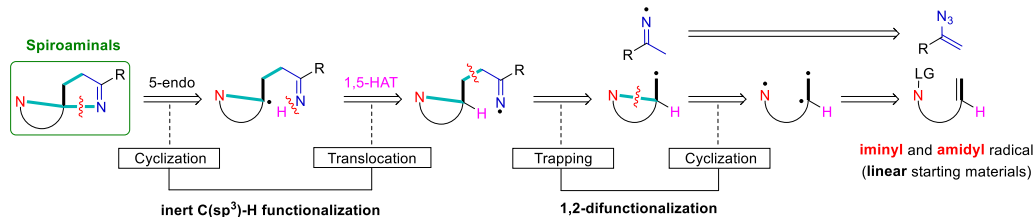
b The existing approaches for the radical-mediated spirocyclization



c alkene multifunctionalization



d This work: nitrogen radical-triggered trifunctionalizing *ipso*-spirocyclization of unactivated alkenes with vinyl azides



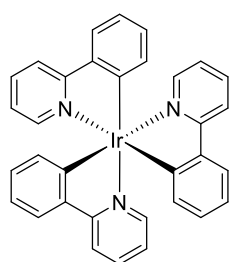
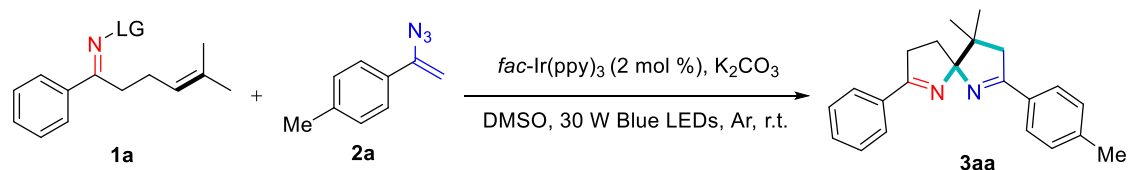
- * Architecturally new spiroaminal frameworks
- * Non-dearomative spirocyclization of linear precursors
- * Alkene trifunctionalization
- * Unactivated alkene: 1,2,n-tri-radical synthon
- * One C-C bond and two geminal C-N bonds in 1-step
- * 52 examples, up to 80% yield
- * Broad substrate scope
- * Good functional group compatibility
- * Easy scalability
- * Product derivatization
- * Late-stage functionalization
- * DFT calculation

Fig. 1 a Representative examples of spirocyclic compounds: natural products, bioactive molecules, and ligands. **b** The existing approaches for the radical-mediated spirocyclization. **c** Different approaches for the multifunctionalization of alkenes. **d** This work: nitrogen radical-triggered trifunctionalizing *ipso*-spirocyclization of unactivated alkenes with vinyl azides.

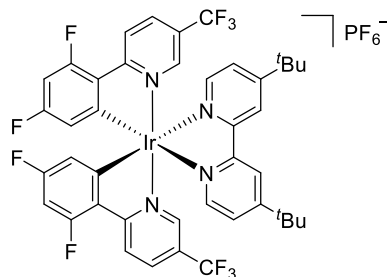
Results

Reaction optimization. To test the described hypothesis, iminyl radical precursor *O*-4-trifluoromethylbenzoyl oxime ester **1a** and vinyl azide **2a** were initially chosen as the model substrates to explore the reaction conditions (Table 1). Unless otherwise noted, all the experiments were performed in the presence of *fac*-Ir(ppy)₃ as photocatalyst, K₂CO₃ as base, and DMSO as solvent under argon atmosphere upon irradiation of 30 W blue light-emitting diodes (LEDs) at room temperature. To our delight, after systematic optimization of the reaction parameters, including nitrogen radical precursors, photocatalyst, solvent, and base, the desired product spirobi[pyrroline] **3aa** was obtained in 71% isolated yield. Based on the more oxidizing ability of electron-deficient *O*-substituted oxime esters, the utilization of other leaving groups (LG) instead of OBz^{CF₃} gave no better results (entries 2 and 3). Among the catalysts examined, *fac*-Ir(ppy)₃ was found to be more effective than other photocatalysts (entries 4 and 5). Furthermore, screening of solvents demonstrated that other solvents delivered no more significant improvement than that of DMSO (entries 6–8). It was worth mentioning that the yields of the desired product declined slightly when the reaction was conducted without the addition of base or argon protection (entries 9 and 10). As anticipated, no desired product could be detected without either light or photocatalyst, indicating the indispensability of both light and photocatalyst in such photocatalytic CTTC cascade (entry 11).

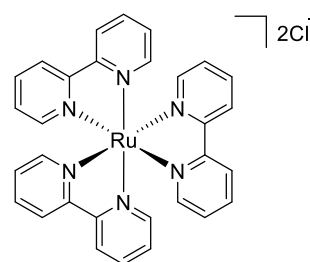
Table 1 Optimization of reaction conditions^a



fac-Ir(ppy)₃ (1)



Ir(dFCF₃ppy)₂(dtbbpy)PF₆ (2)



Ru(bpy)₃Cl₂ (3)

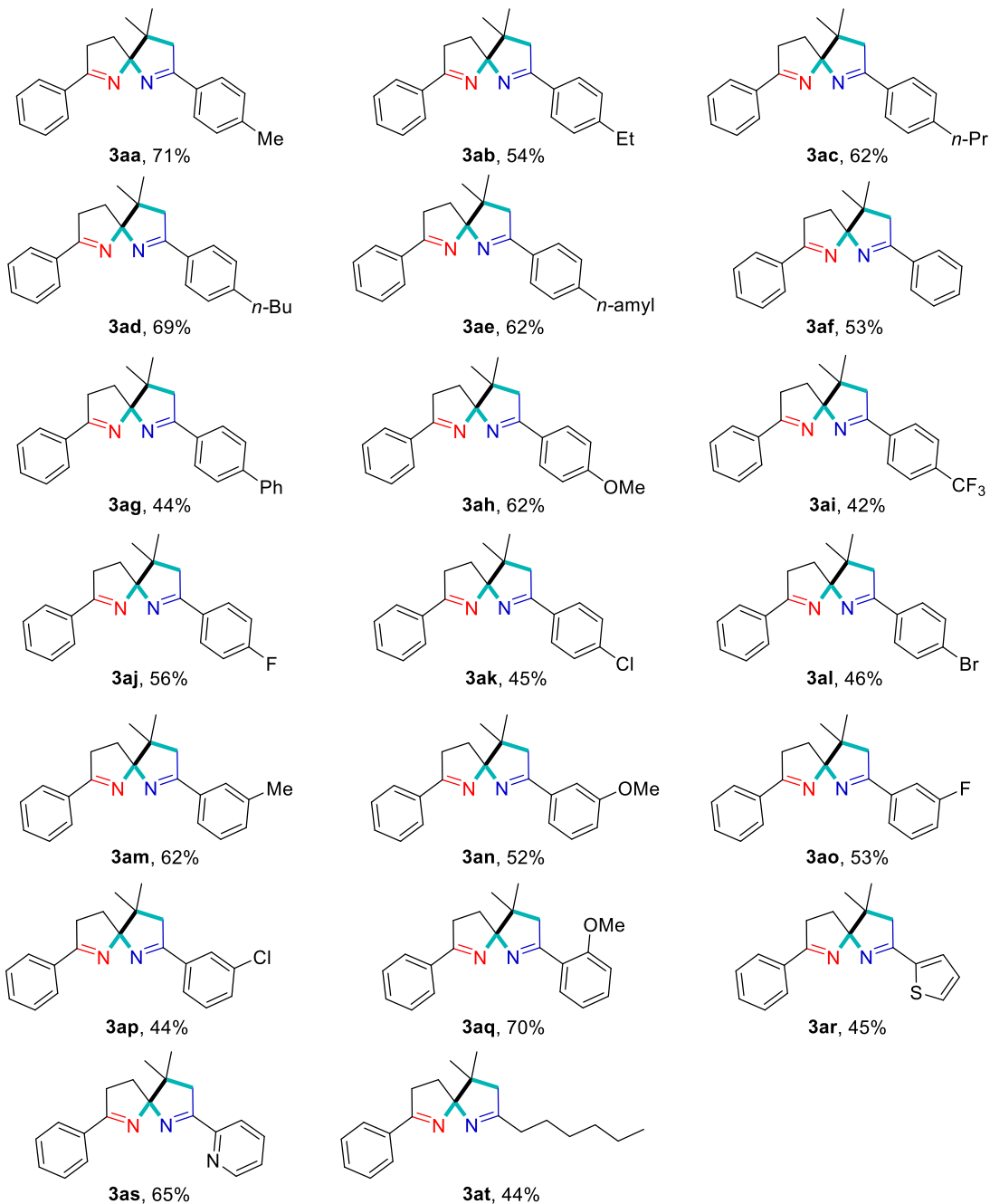
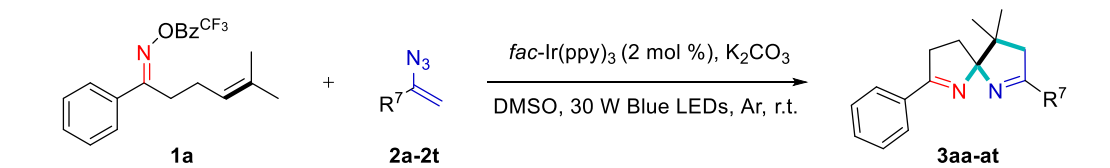
Entry	Variation from the standard conditions	Yield (%) ^b
1	none	76 (71)
2	LG = C ₆ F ₅ CO ₂ -	10
3	LG = 2,4-NO ₂ -C ₆ H ₃ O-	n.d.
4	PC-2 instead of <i>fac</i> -Ir(ppy) ₃	30
5	PC-3 instead of <i>fac</i> -Ir(ppy) ₃	n.d.
6	DMF instead of DMSO	34
7	MeCN instead of DMSO	46
8	DME or MeOH instead of DMSO	n.d.
9	no base	54
10	no argon protection	53
11	no light or photocatalyst	n.d.

^aReaction conditions: **1a** (0.1 mmol), **2a** (0.25 mmol), *fac*-Ir(ppy)₃ (2 mol %), K₂CO₃ (0.15 mmol), DMSO (1 mL), 30 W blue LEDs, argon atmosphere, r.t., 6 h, in a sealed tube. n.d. = no detection. LG = *p*-CF₃-C₆H₄CO₂- (OBz^{CF3}). ^bYields were determined by ¹H NMR using dibromomethane as an internal standard. Isolated yields in parentheses.

Substrate scope on the vinyl azides. With the optimized reaction conditions in hand, we next sought to investigate the substrate scope on the trifunctionalizing *ipso*-spirocyclization enabled by the iminyl radical-triggered CTTC cascade (Table 2). First, the generality of this *ipso*-spirocyclization with regard to vinyl azides was examined with olefinic oxime ester **1a** as the iminyl radical precursor. A variety of vinyl azides with different electronic groups at the *para*- (**3aa–3al**), *meta*- (**3am–3ap**), or *ortho*-position (**3aq**) of the phenyl rings reacted smoothly with **1a** to afford the corresponding spirobi[pyrrolines] in acceptable yields. Gratifyingly, this photocatalytic

trifunctionalizing *ipso*-spirocyclization tolerated a broad range of diverse functionalities such as alkyl (**3aa–3ae**, and **3am**), phenyl (**3ag**), methoxyl (**3ah**, **3an**, and **3aq**), and trifluoromethyl (**3ai**), as well as halogen (**3aj–3al**, **3ao**, and **3ap**) which could be employed as a handle for further derivatization. Furthermore, heteroaryl-substituted vinyl azides including thiophene (**3ar**) and pyridine (**3as**) displayed good reactivity in our protocol. Notably, alkyl-substituted vinyl azide was also proved to be suitable substrate for this spirocyclization and provided 44% yield of the expected spirobi[pyrroline] **3at**.

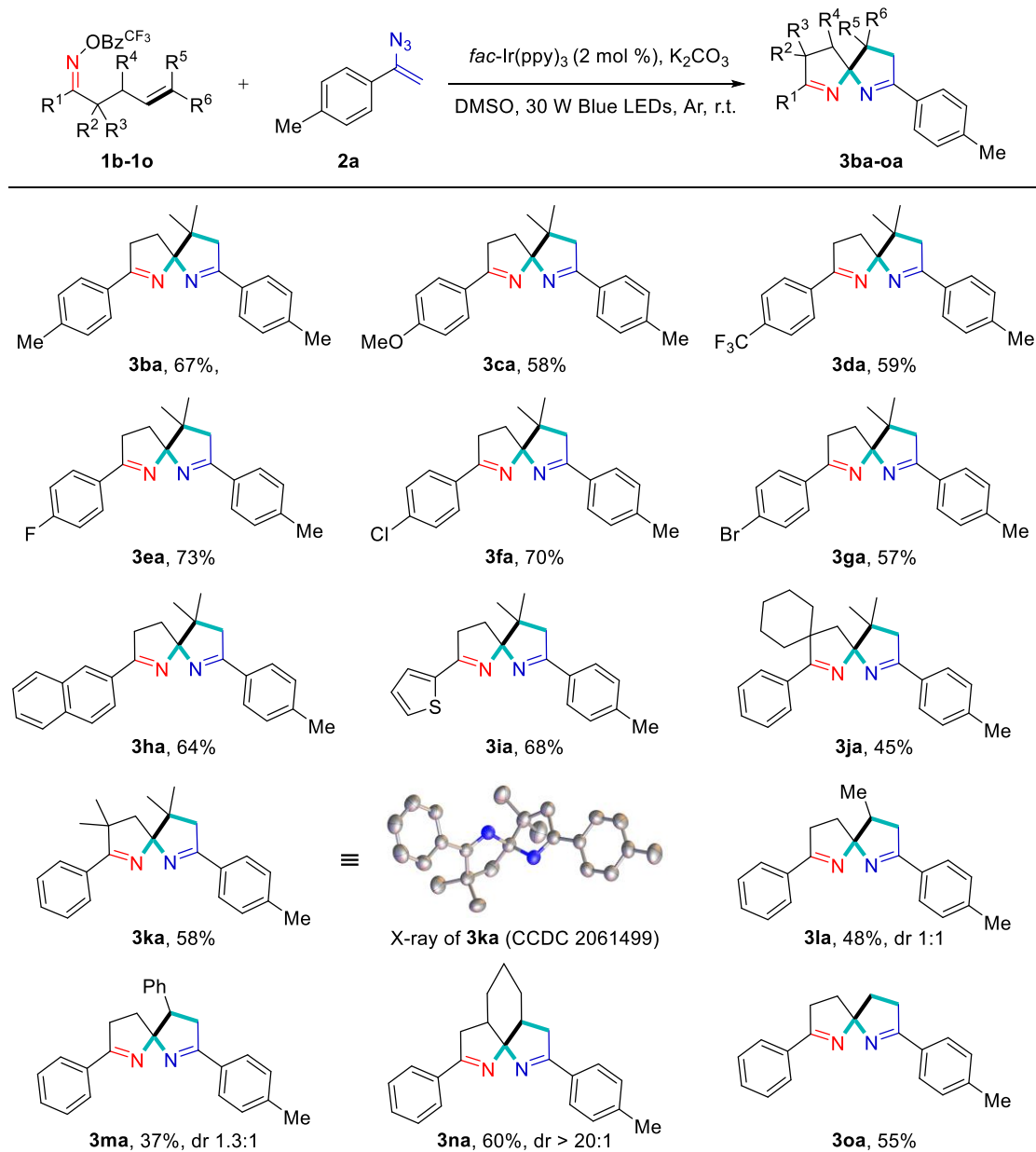
Table 2 Substrate scope on the vinyl azides.^a



^aReaction conditions: **1** (0.2 mmol), **2** (0.5 mmol), *fac*-Ir(ppy)₃ (2 mol %), K₂CO₃ (0.3 mmol), DMSO (2 mL), 30 W blue LEDs, argon atmosphere, r.t., 6 h, in a sealed tube; isolated yields based on **1** after the chromatographic purification.

Substrate scope on the olefinic oxime esters. Having demonstrated the varied functional group compatibility in the vinyl azide coupling partners, we subsequently set out to explore the scope of olefinic oxime esters **1** with **2a** as the coupling partner. As illustrated in Table 3, a panel of aromatic oxime esters bearing electronic variation on the phen rings were also well-tolerated in this transformation, affording the corresponding spirobi[pyrrolines] **3ba–3ga** in moderate to good yields. Furthermore, 2-naphthyl- (**3ha**) and heteroaryl-substituted oxime esters (**3ia**) were also subjected to the present protocol. Additionally, aromatic oxime esters with alkyl chain units at the α position were used as the substrates in this protocol and smoothly transformed into the corresponding spirobi[pyrrolines] **3ja** and **3ka** in 45% and 58% isolated yields, respectively. Notably, the structure of **3ka** was unambiguously confirmed by X-ray crystallographic analysis (CCDC 2061499). Importantly, in addition to 1,2,2-trisubstituted olefinic oxime esters, 1,2-disubstituted (**3la–3na**) and 1-substituted olefinic oxime esters (**3oa**) could also be employed as competent substrates in this transformation to provide the desired products.

Table 3 Substrate scope on the olefinic oxime esters.^a

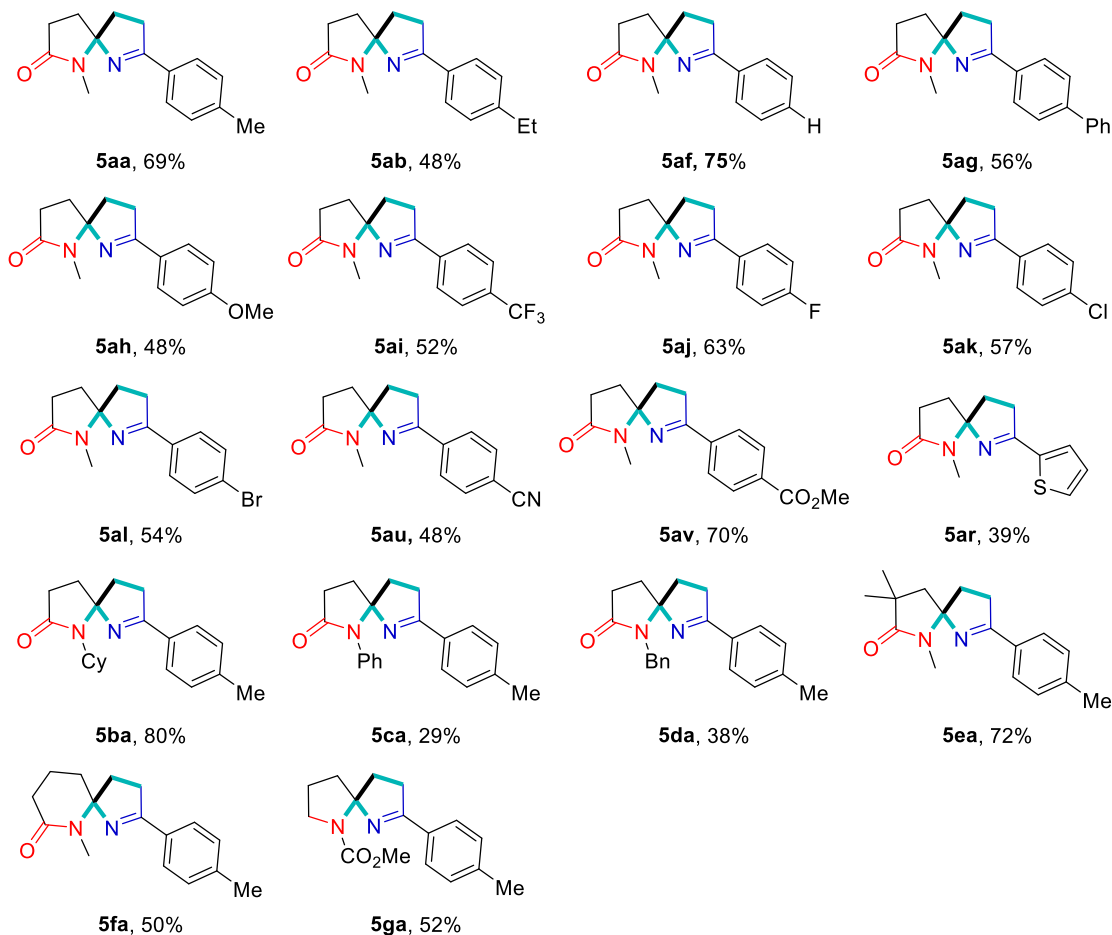
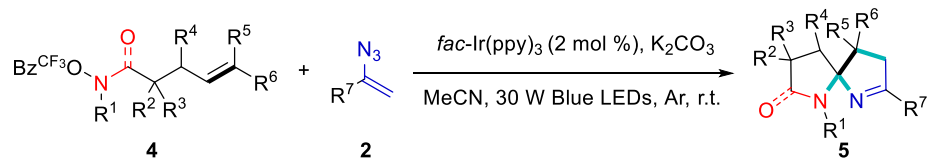


^aReaction conditions: **1** (0.2 mmol), **2** (0.5 mmol), *fac*-Ir(ppy)₃ (2 mol %), K₂CO₃ (0.3 mmol), DMSO (2 mL), 30 W blue LEDs, argon atmosphere, r.t., 6 h, in a sealed tube; isolated yields based on **1** after the chromatographic purification.

Substrate scope on the amidyl radical-triggered trifunctionalizing *ipso*-spirocyclization. Encouraged by the success of the unprecedented trifunctionalizing *ipso*-spirocyclization enabled by the iminyl radical-triggered CTTC cascade, we speculated that the high electrophilic amidyl radical^{41,42} could also trigger such CTTC cascade to achieve the desired trifunctionalizing *ipso*-spirocyclization of

unactivated alkenes for rapid construction of another new spiroaminal framework. Excitingly, upon the facile screening of parameters, amidyl radical precursor olefinic amides were indeed capable partners and readily underwent such photocatalytic trifunctionalizing *ipso*-spirocyclization (Table 4). Similarly, vinyl azides with various electron-donating or electron-withdrawing groups reacted smoothly with **4a** to furnish the structurally novel spiropyrroline lactams in satisfactory yields. Olefinic amides with a hindered *N*-Cy group (**5ba**), *N*-Ph group (**5ca**), as well as a removable *N*-Bn group (**5da**) could successfully participate in this trifunctionalizing *ipso*-spirocyclization. Furthermore, olefinic amide with alkyl chain unit at the α position could be applied as well to deliver the corresponding product **5ea**. In addition, the proposed approach could address 6-*exo-trig* cyclization of unactivated alkene to generate 6-membered ring lactam **5fa**. Interestingly, *N*-protected amine was compatible with the photoredox catalysis and provided the desired spiropyrroline pyrrolidine **5ga** in moderate yield.

Table 4 Substrate scope on the amidyl radical-triggered trifunctionalizing *ipso*-spirocyclization.^a

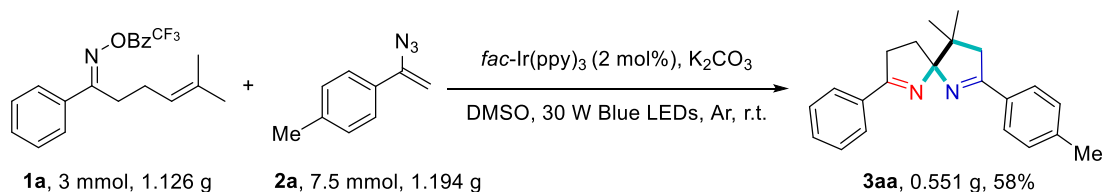


^aReaction conditions: **4** (0.2 mmol), **2** (0.5 mmol), *fac*-Ir(ppy)₃ (2 mol %), K₂CO₃ (0.3 mmol), DMSO (2 mL), 30 W blue LEDs, argon atmosphere, r.t., 6 h, in a sealed tube; isolated yields based on **4** after the chromatographic purification.

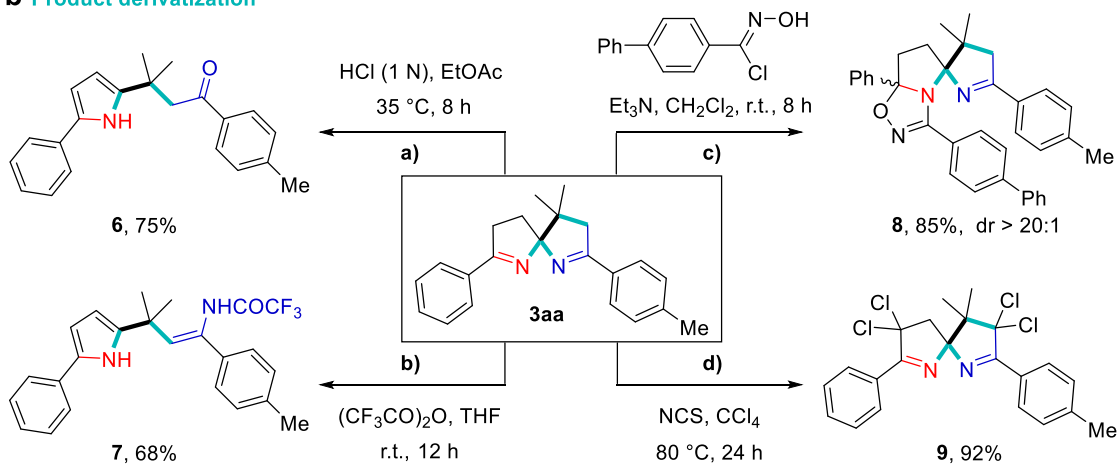
Products transformation. To demonstrate the potential application of the protocol, a gram-scale reaction containing 3.0 mmol of oxime ester **1a** was performed under the standard conditions to afford the target product **3aa** with a satisfactory isolated yield, demonstrating the synthetic practicality and scalability of our photocatalytic trifunctionalizing *ipso*-spirocyclization (Fig. 2a). Moreover, the synthetic utility of the method was further confirmed by facile derivatization of the formed spirobi[pyrroline] **3aa** to yield structurally diverse and valuable molecules (Fig. 2b). Rather surprisingly,

in the presence of protonic acid or trifluoroacetic anhydride, **3aa** can be smoothly transformed into the aromatized 1*H*-pyrrole derivatives (**6** and **7**) in 75% and 68% yields, respectively. Moreover, [3 + 2] cycloaddition reaction between **3aa** and *N*-hydroxybenzimidoyl chloride allowed access to the 1,2,4-oxadiazoline-fused sipropryrroline **8**. When spirobi[pyrroline] **3aa** was treated with *N*-chlorosuccinimide (NCS) at 80 °C for 24 h, the multi-halogen-substituted spiroaminal **9** was obtained with excellent isolated yield. Delightfully, estrone-derived vinyl azide **2w** readily engaged in such photocatalytic transformation with olefinic oxime ester **1a** to give the structurally more complex and intriguing compound **3aw**, demonstrating the potential application of this methodology (Fig. 2c). Additionally, when 1,1-disubstituted terminal olefinic oxime esters were subjected to the reaction system, the desired 1,5-HAT process did not proceed smoothly and thus no corresponding spirobi[pyrroline] was detected. Interestingly, using vinyl azide 2-azidoallyl diphenylmethyl ether **2x** as the coupling partner, the second iminyl radical derived from vinyl azide underwent intramolecular 1,5-HAT (from nitrogen to benzyl carbon atom) and further cyclization to afford a panel of the oxazoline-based pyrrolines **10px–10ux** (Fig. 2d). Notably, terminal olefinic oxime ester **1o** could also be converted into the expected oxazoline-based pyrroline **10ox** albeit with somewhat low yield.

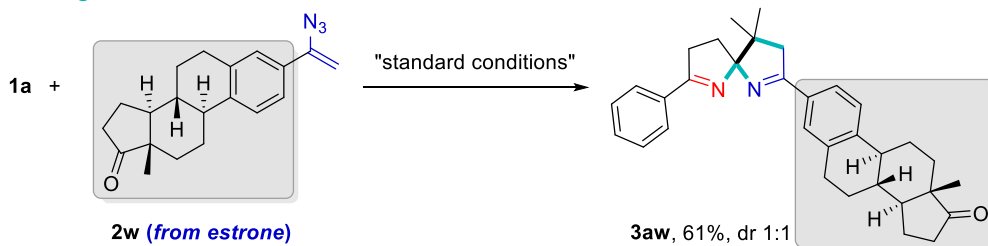
a Gram-scale reaction



b Product derivatization



c Late-stage functionalization



d Exploration of other vinyl azides and olefinic oxime esters

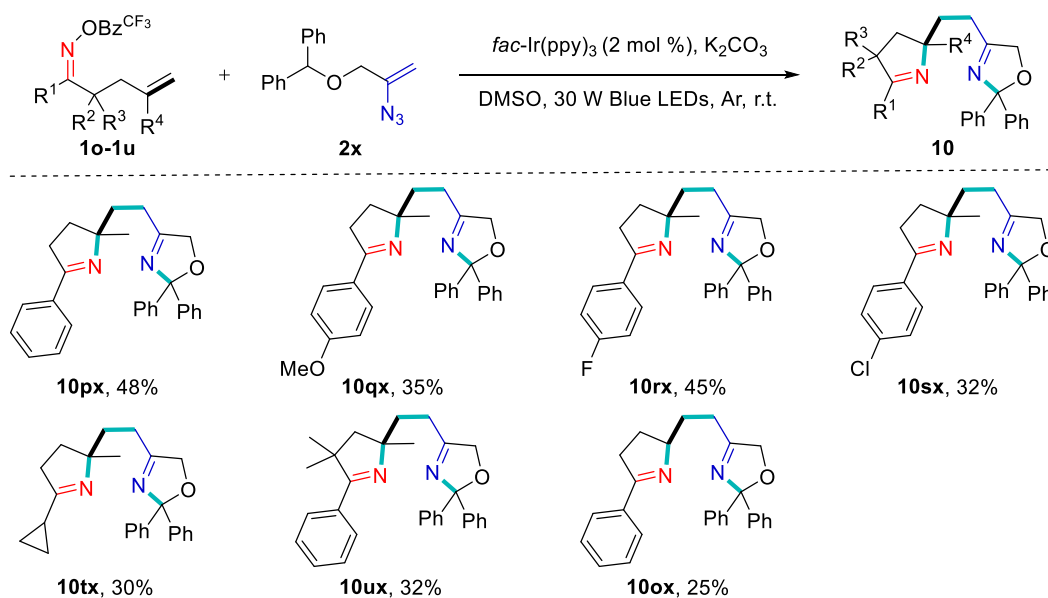
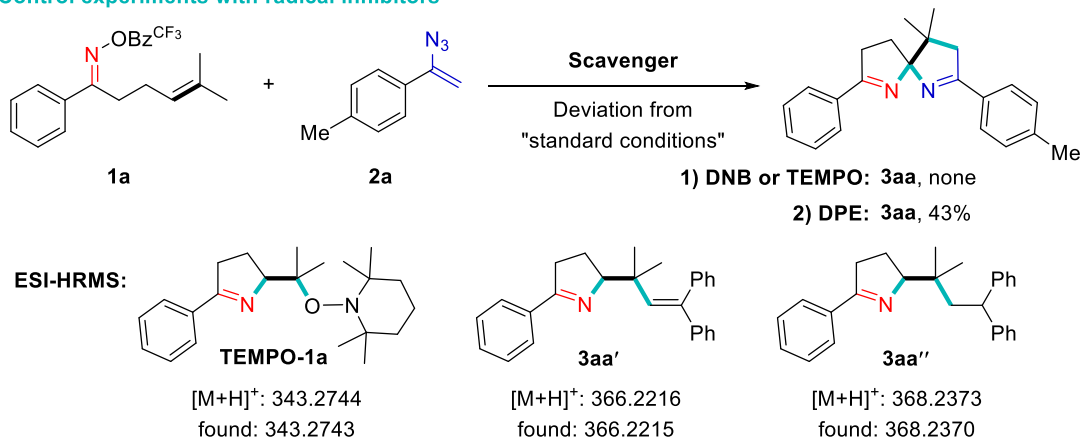


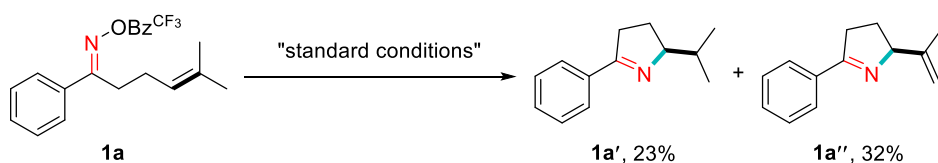
Fig. 2 Gram-scale synthesis and synthetic applications of the reaction.

Mechanistic studies. To rationalize the mechanism of this photocatalytic trifunctionalizing *ipso*-spirocyclization reaction, several control experiments were carried out. As shown in Scheme 3, upon the addition of electron-transfer scavenger p-dinitrobenzene (DNB) or radical scavenger 2,2,6,6-tetramethyl-piperidinyloxy (TEMPO) into the model reaction, the formation of the desired product **3aa** was completely inhibited (Fig. 3a). And the corresponding **1a**-derived TEMPO-trapped adduct was detected through LC–HRMS analysis. When the model reaction was performed in the presence of quintessential radical-trapping reagent 1,1-diphenylethylene (DPE), the yield of **3aa** declined slightly from 71% to 43%, and the radical-trapping products (**3aa'** and **3aa''**) were detected through LC–HRMS analysis (Fig. 3a). Subsequently, in the absence of vinyl azide **2a**, the hydroimination product **1a'** and olefination product **1a''** were obtained in 23% and 32% yield, respectively (Fig. 3b). These results indicate that not only a single electron transfer (SET)/radical process but also the carbon-radical intermediates generated through iminyl radical-triggered intramolecular cyclization might be involved in the present transformation. Additionally, no desired product **3aa** was detected when vinyl azide **2a** was replaced with 3-phenyl-2*H*-azirine **2a'** generated from the denitrogenative decomposition of vinyl azide under the standard conditions, suggesting that 2*H*-azirine intermediates might be ruled out in this transformation (Fig. 3c).

a Control experiments with radical inhibitors



b Control experiment without the addition of vinyl azide



c Control experiment using 2H-azirine instead of vinyl azide

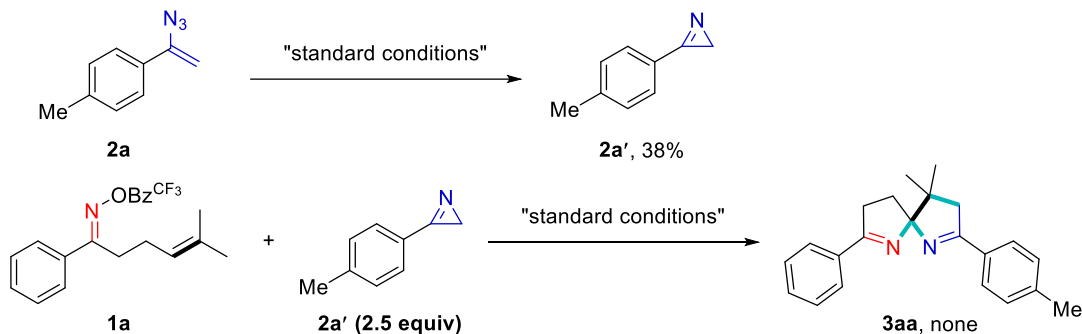


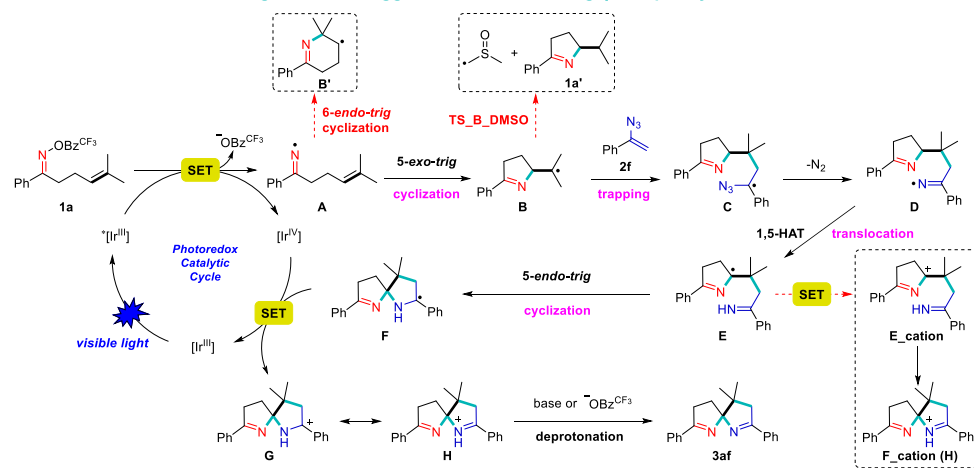
Fig. 3 Preliminary mechanistic studies. **a** Control experiments with radical inhibitors. **b** Control experiment without the addition of vinyl azide. **c** Control experiment using 2*H*-azirine instead of vinyl azide.

On the basis of the above-mentioned results and preceding reports⁴³⁻⁴⁵, a photoinduced electron transfer (PET) mechanism was proposed for the trifunctionalizing *ipso*-spirocyclization. Density functional theory (DFT) calculations were also carried out to further validate the proposed reaction mechanism and the factors governing chemoselectivity at the M06-2X/def2-TZVP/SMD(DMSO)//M06-2X/def2-SVP level of theory⁴⁶⁻⁵². As illustrated in Fig. 4, the oxime ester **1a** ($E_{1/2}^{\text{red}} = -1.61$ V vs. SCE, see the Supporting

Information) can undergo exergonic single-electron transfer (SET) process (42.4 kcal mol⁻¹) with the excited *Ir^{III} [$E_{1/2}^{\text{red}}(\text{Ir}^{\text{IV}}/*\text{Ir}^{\text{III}}) = -1.73 \text{ V vs. SCE}$]⁵³ to deliver the first iminyl radical **A**, which could go through thermodynamically favorable intramolecular 5-*exo-trig* cyclization to generate the first pyrroline species **B** containing an alkyl radical. Alternatively, the 6-*endo-trig* cyclization pathway is kinetically less favored ($\text{TS}_{6\text{-endo-trig}} = 18.66 \text{ kcal mol}^{-1}$ vs. $\text{TS}_{5\text{-exo-trig}} = 11.61 \text{ kcal mol}^{-1}$). Two possible pathways were expected for the following reaction pathway of **B**, including intermolecular radical trapping with vinyl azide **2f** (black line) and hydrogen atom abstraction with the C-H of solvent dimethyl sulfoxide (red line). DFT calculations determined that the activation free energy of the addition of carbon radical intermediate **B** to the C=C of **2f** was only 5.98 kcal mol⁻¹, which was much lower than that who was found for the pathway *via* **TS_B_DMSO** (25.55 kcal mol⁻¹). This radical trapping would create a new C-C bond in α -azide benzyl radical **C**, which is an exergonic process (23.74 kcal mol⁻¹). Next, the α -azide benzyl radical **C** could rapidly release a N₂ molecule *via* an almost barrierless transition state (**TS_C**, 0.19 kcal mol⁻¹) after conformation adjustment to the isomer **C(2)** and thus result in the formation of the second imine radical **D**. The iminyl radical **D** underwent a radical translocation process of 1,5-HAT *via* transition state **TS_D_E** with a moderate energy barrier of 11.05 kcal mol⁻¹ to generate a more stabilized α -amino carbon radical **E(1)**. Then, an intramolecular 5-*endo-trig* cyclization with an imine moiety led to the second pyrroline species **F** containing a benzyl radical with the highest energy barrier 18.95 kcal mol⁻¹ in the whole trifunctionalizing *ipso*-spirocyclization reaction, indicating that the radical cyclization process is the rate-limiting step in the reaction. Subsequently, the intermediate **F** (calculated $E_{1/2}^{\text{ox}} = -1.15 \text{ V vs. SCE}$) can be easily oxidized by Ir^{IV} [$E_{1/2}^{\text{red}}(\text{Ir}^{\text{IV}}/\text{Ir}^{\text{III}}) = 0.77 \text{ V vs. SCE}$] to the carbon cation **G**, which could resonate to the protonated product **H**. Finally, the target spirobi[pyrroline] **3af** could be obtained after the deprotonation of compound **H** with the help of *p*-trifluoromethylbenzoate anion or base. Although the reaction pathway of the oxidation of radical intermediate **E** (calculated $E_{1/2}^{\text{ox}} = -0.15 \text{ V vs. SCE}$) to intermediate **E_cation** by oxidative Ir^{IV} complex could be envisioned, the efforts aiming to locate the transition state of

intramolecular ionic cyclization of intermediate **E_cation** leading to intermediate **H** has been failed.

a Proposed mechanism for the nitrogen radical-triggered trifunctionalizing ipso-spirocyclization



b Free energy profiles for the the nitrogen radical-triggered trifunctionalizing ipso-spirocyclization

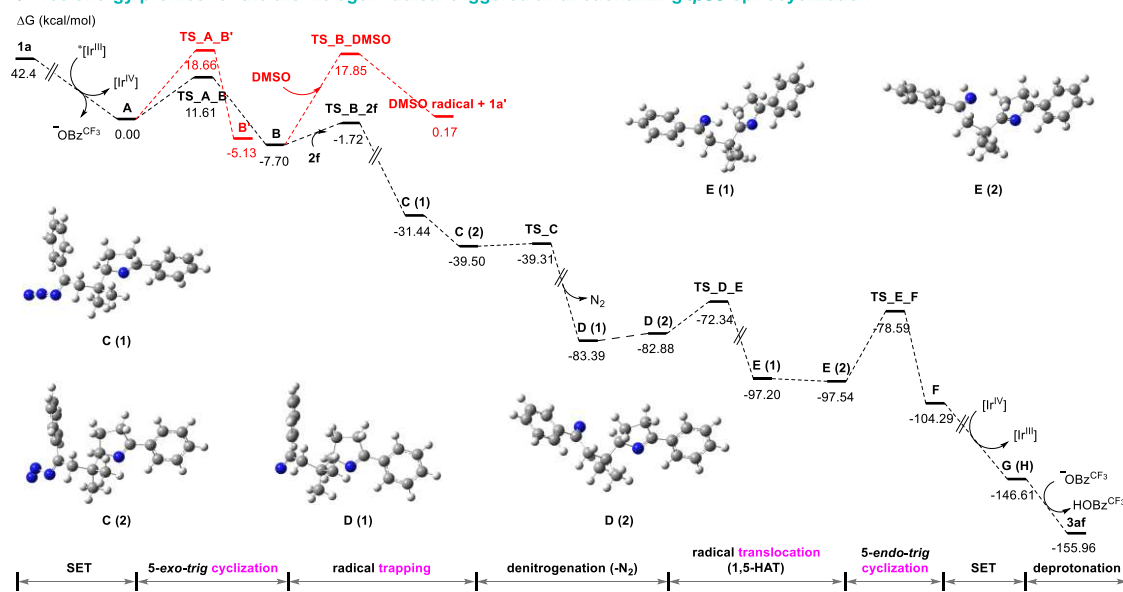


Fig. 4 Proposed mechanism and free energy profiles for the nitrogen radical-triggered trifunctionalizing *ipso*-spirocyclization of unactivated alkenes. The values have been given in the unit of kcal mol⁻¹ and represent the relative free energies calculated using M06-2X method in DMSO solvent. Note: Two different energy values for one structure refer to conformer changes.

Discussion

In conclusion, we successfully developed a novel, selective, and efficient strategy to realize trifunctionalizing *ipso*-spirocyclization of unactivated internal and terminal alkenes by photoredox-catalyzed, nitrogen radical-triggered relay cascade involving

1,5-HAT, which would open up a new reaction mode of alkenes. Not only iminyl radical precursor olefinic oxime esters but also amidyl radical precursor olefinic amides are subjected to the developed photocatalytic protocol, allowing a rapid and efficient entry to a diverse array of architecturally new and intriguing spiroaminal frameworks through the simultaneous formation of one C–C bond and two geminal C–N bonds. Furthermore, the resulting spiroaminals can be diversely functionalized through various facile transformations, such as aromatization into 2,5-disubstituted pyrroles, [3 + 2] cyclization, and multi-halogenation reaction. And the applicability of such protocol is also demonstrated by late-stage functionalization of bioactive estrone derivative. In addition, the mechanistic studies indicate that this transformation undergoes a nitrogen radical-triggered cyclization-trapping-translocation-cyclization (CTTC) cascade, namely intramolecular 5-*exo-trig* cyclization, intermolecular radical trapping, 1,5-HAT, and 5-*endo-trig* cyclization. Further application of this strategy is currently underway in our laboratory.

Methods

General procedure. An oven-dried Schlenk tube (10 mL) equipped with a stirring bar was charged with olefinic oxime ester **1** (0.2 mmol, 1.0 equiv.), K₂CO₃ (0.3 mmol, 1.5 equiv.), and *fac*-Ir(ppy)₃ (2 mol%). The tube was connected to a vacuum line where it was evacuated and back-filled with Ar for three times. Next, vinyl azide **2** (0.5 mmol, 2.5 equiv.) and DMSO (2 mL) were added under Ar flow. The tube was placed approximately 2 cm from 30 W blue LEDs, and then stirred at room temperature for 6 h. After completion, the reaction was quenched with H₂O (4.5 mL) and extracted with EtOAc. The organic layer was washed with saturated brine and dried over Na₂SO₄. The solvent was removed under reduced pressure, and the resulting residue was purified by column chromatography on silica gel to afford the desired product **3**. **Note:** for olefinic amides **4** (MeCN was used instead of DMSO), the reaction mixture was filtered after completion, concentrated under reduced pressure, and purified by column chromatography on silica gel to afford the desired product **5**.

Additional Information

Supplemental Information can be found with this article online. The crystallography data have been deposited at the Cambridge Crystallographic Data Center (CCDC) under accession number CCDC: 2061499 (methyl ester of **3ka**) and can be obtained free of charge from

Author contributions

D.Y. and X.D. conceived and designed the study, and wrote the paper. Z.Y.Q., Z.J.Z., L.Y., D.Z. performed the experiments and mechanistic studies. Q.F. and S.P.W. performed the DFT calculations. All authors contributed to the analysis and interpretation of the data.

Acknowledgments

This work was supported by the Scientific Fund of Sichuan Province (21YYJC0697), the Collaborative Fund of Luzhou Government and Southwest Medical University (2018LZXNYD-ZK33, 2018LZXNYD-ZK39, and 2018LZXNYD-ZK04), the Collaborative Fund of Luzhou Municipal Government and Sichuan University (2018CDLZ-13), and the Open Project of Central Nervous System Drug Key Laboratory of Sichuan Province (200023-01SZ). We give thanks to Professor Jing Zeng (School of Pharmacy, SWMU) for assistance in HR-MS.

References

1. Wang, Q., Tang, X. L., Luo, X. C., de Voogd, N. J., Li, P. L. & Li, G. Q. (+)- and (-)-Spiroreticulatine, a pair of unusual spiro bisheterocyclic quinoline-imidazole alkaloids from the south china sea sponge *fascaplysinopsis reticulata*. *Org. Lett.* **17**, 3458-3461 (2015).
2. Hu, J. F., Fan, H., Xiong, J. & Wu, S. B. Discorhabdins and pyrroloiminoquinone-related alkaloids. *Chem. Rev.* **111**, 5465-5491 (2011).
3. Edrada, R. A., Stessman, C. C. & Crews, P. Uniquely modified imidazole alkaloids from a calcareous leucetta sponge. *J. Nat. Prod.* **66**, 939-942 (2003).
4. Chatgililoglu, C., Gimisis, T. & Spada, G. P. C-1' radical-based approaches for the synthesis of anomeric spironucleosides. *Chem. Eur. J.* **5**, 2866-2876 (1999).
5. Pearson, M. S. M., Floquet, N., Bello, C., Vogel, P., Plantier-Royon, R., Szymoniak, J., Bertus, P. & Behr, J.-B. The spirocyclopropyl moiety as a methyl surrogate in the structure of l-fucosidase and l-rhamnosidase inhibitors. *Bioorg. Med. Chem.* **17**, 8020-8026 (2009).
6. White, D. E., Stewart, I. C., Grubbs, R. H. & Stoltz, B. M. The catalytic asymmetric total synthesis of elatol. *J. Am. Chem. Soc.* **130**, 810-+ (2008).
7. Wang, X., Han, Z., Wang, Z. & Ding, K. A type of structurally adaptable aromatic spiroketal based chiral diphosphine ligands in asymmetric catalysis. *Acc. Chem. Res.* **54**, 668-684 (2021).
8. Tian, J. M., Yuan, Y. H., Xie, Y. Y., Zhang, S. Y., Ma, W. Q., Zhang, F. M., Wang, S. H., Zhang, X. M. & Tu, Y. Q. Catalytic asymmetric cascade using spiro-pyrrolidine organocatalyst: efficient construction of hydrophenanthridine derivatives. *Org. Lett.* **19**, 6618-6621 (2017).

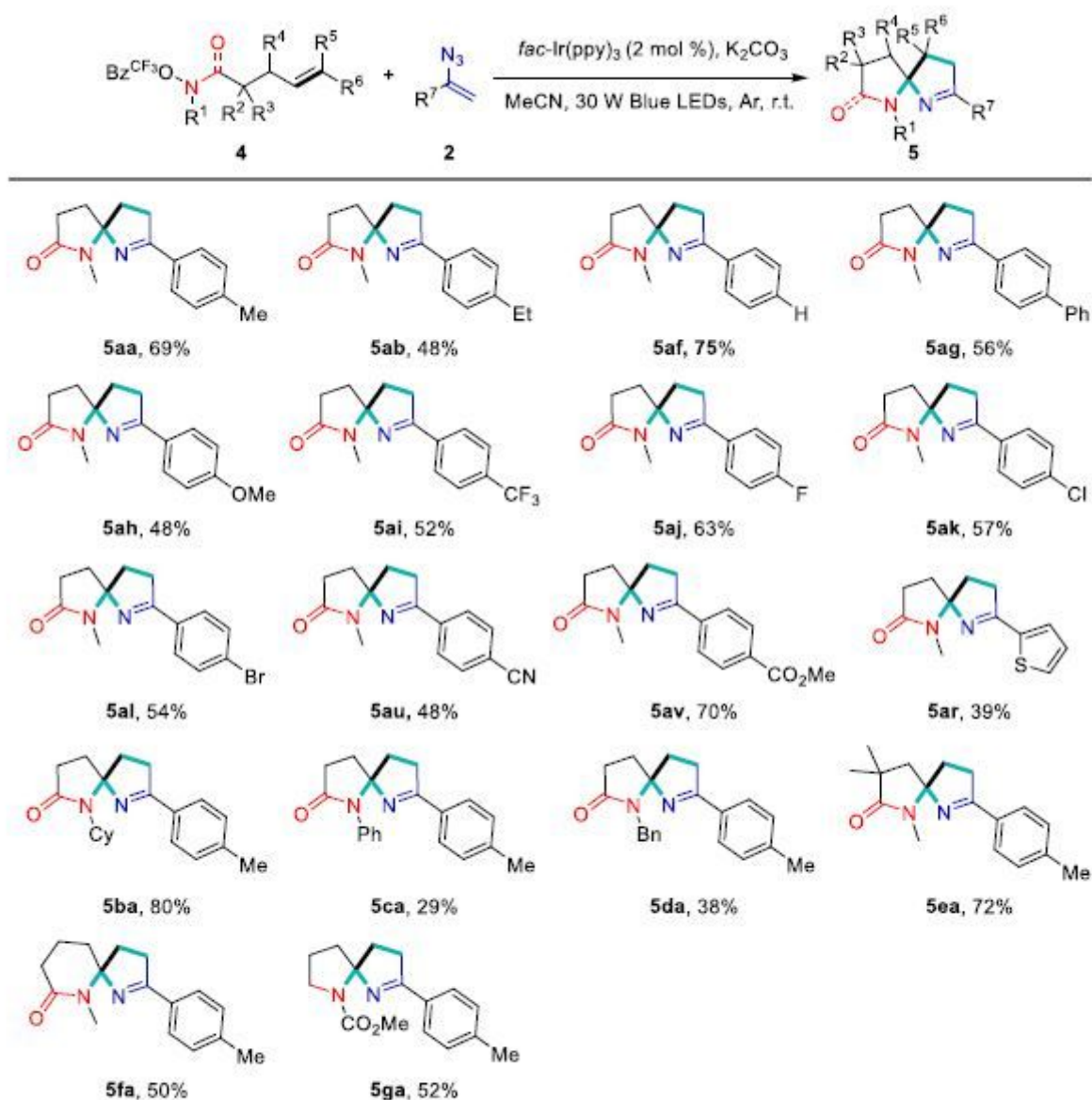
9. Ding, K., Han, Z. & Wang, Z. Spiro skeletons: a Class of privileged structure for chiral ligand design. *Chem. Asian J.* **4**, 32-41 (2009).
10. Xie, J.-H. & Zhou, Q.-L. Chiral diphosphine and monodentate phosphorus ligands on a spiro scaffold for transition-metal-catalyzed asymmetric reactions. *Acc. Chem. Res.* **41**, 581-593 (2008).
11. Dou, Q. Y., Tu, Y. Q., Zhang, Y., Tian, J. M., Zhang, F. M. & Wang, S. H. Spiro-pyrrolidine-catalyzed asymmetric conjugate addition of hydroxylamine to enals and 2,4-dienals. *Adv. Synth. Catal.* **358**, 874-879 (2016).
12. Tian, J. M., Yuan, Y. H., Tu, Y. Q., Zhang, F. M., Zhang, X. B., Zhang, S. H., Wang, S. H. & Zhang, X. M. The design of a spiro-pyrrolidine organocatalyst and its application to catalytic asymmetric Michael addition for the construction of all-carbon quaternary centers. *Chem. Commun.* **51**, 9979-9982 (2015).
13. Yang, W. C., Zhang, M. M. & Feng, J. G. Recent advances in the construction of spiro compounds via radical dearomatization. *Adv. Synth. Catal.* **362**, 4446-4461 (2020).
14. Pawlowski, R., Skorka, P. & Stodulski, M. Radical-mediated non-dearomative strategies in construction of spiro compounds. *Adv. Synth. Catal.* **362**, 4462-4486 (2020).
15. Liu, C., Zeng, H., Zhu, C. & Jiang, H. Recent advances in three-component difunctionalization of gem-difluoroalkenes. *Chem. Commun.* **56**, 10442-10452 (2020).
16. Jiang, H. & Studer, A. Intermolecular radical carboamination of alkenes. *Chem. Soc. Rev.* **49**, 1790-1811 (2020).
17. Lin, J., Song, R.-J., Hu, M. & Li, J.-H. Recent advances in the intermolecular oxidative difunctionalization of alkenes. *Chem. Rec.* **19**, 440-451 (2019).
18. Kaur, N., Wu, F., Alom, N.-E., Ariyaratna, J. P., Saluga, S. J. & Li, W. Intermolecular alkene difunctionalizations for the synthesis of saturated heterocycles. *Org. Biomol. Chem.* **17**, 1643-1654 (2019).
19. Bao, X., Li, J., Jiang, W. & Huo, C. Radical-mediated difunctionalization of styrenes. *Synthesis* **51**, 4507-4530 (2019).
20. Lan, X.-W., Wang, N.-X. & Xing, Y. Recent advances in radical difunctionalization of simple alkenes. *Eur. J. Org. Chem.* **2017**, 5821-5851 (2017).
21. Yang, S., Chen, Y. & Ding, Z. Recent progress of 1,1-difunctionalization of olefins. *Org. Biomol. Chem.* **18**, 6983-7001 (2020).
22. Balaji, P. V. & Chandrasekaran, S. Stereoselective anti-Markovnikov geminal diamination and dioxy-gena-tion of vinylarenes mediated by the bromonium ion. *Eur. J. Org. Chem.* **2016**, 2547-2554 (2016).

23. Elliott, L. D., Wrigglesworth, J. W., Cox, B., Lloyd-Jones, G. C. & Booker-Milburn, K. I. 2,2-Difunctionalization of alkenes via Pd(II)-catalyzed aza-Wacker reactions. *Org. Lett.* **13**, 728-731 (2011).
24. Nenajdenko, V. G., Muzalevskiy, V. M., Shastin, A. V., Balenkova, E. S., Kondrashov, E. V., Ushakov, I. A. & Rulev, A. Y. Fragmentation of trifluoromethylated alkenes and acetylenes by N,N-binucleophiles. Synthesis of imidazolines or imidazolidines (oxazolidines) controlled by substituent. *J. Org. Chem.* **75**, 5679-5688 (2010).
25. Chen, W., Liu, X., Chen, E., Chen, B., Shao, J. & Yu, Y. KI-mediated radical multi-functionalization of vinyl azides: a one-pot and efficient approach to β -keto sulfones and α -halo- β -keto sulfones. *Org. Chem. Front.* **4**, 1162-1166 (2017).
26. Huang, S., Thirupathi, N., Tung, C.-H. & Xu, Z. Copper-catalyzed oxidative trifunctionalization of olefins: an access to functionalized β -keto thiosulfones. *J. Org. Chem.* **83**, 9449-9455 (2018).
27. Liang, W., Jiang, K., Du, F., Yang, J., Shuai, L., Ouyang, Q., Chen, Y.-C. & Wei, Y. Iron-catalyzed, iminyl radical-triggered cascade 1,5-hydrogen atom transfer/(5+2) or (5+1) annulation: oxime as a five-atom assembling unit. *Angew. Chem. Int. Ed.* **59**, 19222-19228 (2020).
28. Kumar, G., Pradhan, S. & Chatterjee, I. N-centered radical directed remote C-H bond functionalization via hydrogen atom transfer. *Chem. Asian J.* **15**, 651-672 (2020).
29. Chen, H. & Yu, S. Remote C-C bond formation via visible light photoredox-catalyzed intramolecular hydrogen atom transfer. *Org. Biomol. Chem.* **18**, 4519-4532 (2020).
30. Shu, W. & Nevado, C. Visible-light-mediated remote aliphatic C-H functionalizations through a 1,5-hydrogen transfer cascade. *Angew. Chem. Int. Ed.* **56**, 1881-1884 (2017).
31. Shu, W., Lorente, A., Gomez-Bengoia, E. & Nevado, C. Expedient diastereoselective synthesis of elaborated ketones via remote Csp³-H functionalization. *Nat. Commun.* **8**, 13832pp. (2017).
32. Tang, Y.-Q., Yang, J.-C., Wang, L., Fan, M. & Guo, L.-N. Ni-catalyzed redox-neutral ring-opening/radical addition/ring-closing cascade of cycloketone oxime esters and vinyl azides. *Org. Lett.* **21**, 5178-5182 (2019).
33. Terhorst, S., Tiwari, D. P., Meister, D., Petran, B., Rissanen, K. & Bolm, C. Syntheses of trifluoroethylated N-heterocycles from vinyl azides and Togni's reagent involving 1,n-hydrogen-atom transfer reactions. *Org. Lett.*, (2020).
34. Liao, Y., Ran, Y., Liu, G., Liu, P. & Liu, X. Transition-metal-free radical relay cyclization of vinyl azides with 1,4-dihydropyridines involving a 1,5-hydrogen-atom transfer: access to α -tetralone scaffolds. *Org. Chem. Front.* **7**, 3638-3647 (2020).
35. Xiao, W. & Wu, J. Recent advances for the photoinduced CC bond cleavage of cycloketone oximes. *Chin. Chem. Lett.* **31**, 3083-3094 (2020).

36. Wang, P., Zhao, Q., Xiao, W. & Chen, J. Recent advances in visible-light photoredox-catalyzed nitrogen radical cyclization. *Green Synth. Catal.* **1**, 42-51 (2020).
37. Yin, W. & Wang, X. Recent advances in iminyl radical-mediated catalytic cyclizations and ring-opening reactions. *New J. Chem.* **43**, 3254-3264 (2019).
38. Jiang, H. & Studer, A. Chemistry with N-centered radicals generated by single-electron transfer-oxidation using photoredox catalysis. *CCS Chem.* **1**, 38-49 (2019).
39. Zhao, Y. & Xia, W. Recent advances in radical-based C–N bond formation via photo-/electrochemistry. *Chem. Soc. Rev.* **47**, 2591-2608 (2018).
40. Davies, J., Morcillo, S. P., Douglas, J. J. & Leonori, D. Hydroxylamine derivatives as nitrogen-radical precursors in visible-light photochemistry. *Chem. Eur. J.* **24**, 12154-12163 (2018).
41. Angelini, L., Davies, J., Simonetti, M., Malet Sanz, L., Sheikh, N. S. & Leonori, D. Reaction of nitrogen-radicals with organometallics under Ni-catalysis: N-arylations and amino-functionalization cascades. *Angew. Chem. Int. Ed.* **58**, 5003-5007 (2019).
42. Davies, J., Svejstrup, T. D., Fernandez Reina, D., Sheikh, N. S. & Leonori, D. Visible-light-mediated synthesis of amidyl radicals: transition-metal-free hydroamination and N-arylation reactions. *J. Am. Chem. Soc.* **138**, 8092-8095 (2016).
43. Wu, C., Liu, T.-X., Zhang, P., Zhu, X. & Zhang, G. Iron-catalyzed redox-neutral radical cascade reaction of [60]fullerene with γ,δ -unsaturated oxime esters: preparation of free (N–H) pyrrolidino[2',3':1,2]fullerenes. *Org. Lett.* **22**, 7327-7332 (2020).
44. Shimbayashi, T., Nakamoto, D., Okamoto, K. & Ohe, K. Facile construction of tetrahydropyrrolizines by iron-catalyzed double cyclization of alkene-tethered oxime esters with 1,2-disubstituted alkenes. *Org. Lett.* **20**, 3044-3048 (2018).
45. Cai, S.-H., Xie, J.-H., Song, S., Ye, L., Feng, C. & Loh, T.-P. Visible-light-promoted carboimination of unactivated alkenes for the synthesis of densely functionalized pyrroline derivatives. *ACS Catal.* **6**, 5571-5574 (2016).
46. The M06 level of theory: Zhao, Y. & Truhlar, D. G. The M06 suite of density functionals for main group thermochemistry, thermochemical kinetics, noncovalent interactions, excited states, and transition elements: two new functionals and systematic testing of four M06-class functionals and 12 other functionals. *Theor. Chem. Acc.* **120**, 215-241 (2008).
47. The def2-svp and def2-tzvp level of theory: Pritchard, B. P., Altarawy, D., Didier, B., Gibson, T. D. & Windus, T. L. New basis set exchange: an open, up-to-date resource for the molecular sciences community. *J. Chem. Inf. Model.* **59**, 4814-4820 (2019).

48. The def2-svp and def2-tzvp level of theory: Schuchardt, K. L., Didier, B. T., Elsethagen, T., Sun, L., Gurumoorthi, V., Chase, J., Li, J. & Windus, T. L. Basis set exchange: a community database for computational sciences. *J. Chem. Inf. Model.* **47**, 1045-1052 (2007).
49. The def2-svp and def2-tzvp level of theory: Weigend, F. & Ahlrichs, R. Balanced basis sets of split valence, triple zeta valence and quadruple zeta valence quality for H to Rn: Design and assessment of accuracy. *Phys. Chem. Chem. Phys.* **7**, 3297-3305 (2005).
50. The def2-svp and def2-tzvp level of theory: Feller, D. The role of databases in support of computational chemistry calculations. *J. Comput. Chem.* **17**, 1571-1586 (1996).
51. The def2-svp and def2-tzvp level of theory: Andrae, D., Häußermann, U., Dolg, M., Stoll, H. & Preuß, H. Energy-adjusted ab initio pseudopotentials for the second and third row transition elements. *Theor. Chim. Acta* **77**, 123-141 (1990).
52. The SMD level of theory: Marenich, A. V., Cramer, C. J. & Truhlar, D. G. Universal solvation model based on solute electron density and on a continuum model of the solvent defined by the bulk dielectric constant and atomic surface tensions. *J. Phys. Chem. B* **113**, 6378-6396 (2009).
53. Nguyen, J. D., D'Amato, E. M., Narayanam, J. M. R. & Stephenson, C. R. J. Engaging unactivated alkyl, alkenyl and aryl iodides in visible-light-mediated free radical reactions. *Nat. Chem.* **4**, 854-859 (2012).

Figures

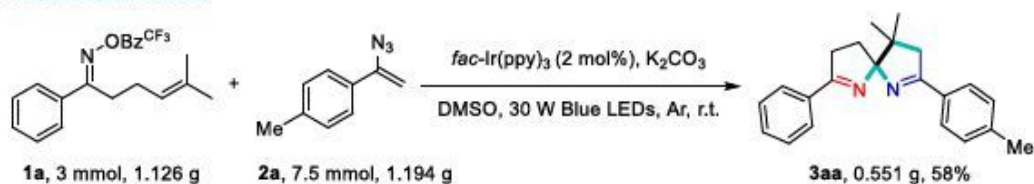


^aReaction conditions: **4** (0.2 mmol), **2** (0.5 mmol), *fac*-Ir(ppy)₃ (2 mol %), K₂CO₃ (0.3 mmol), DMSO (2 mL), 30 W blue LEDs, argon atmosphere, r.t., 6 h, in a sealed tube; isolated yields based on **4** after the chromatographic purification.

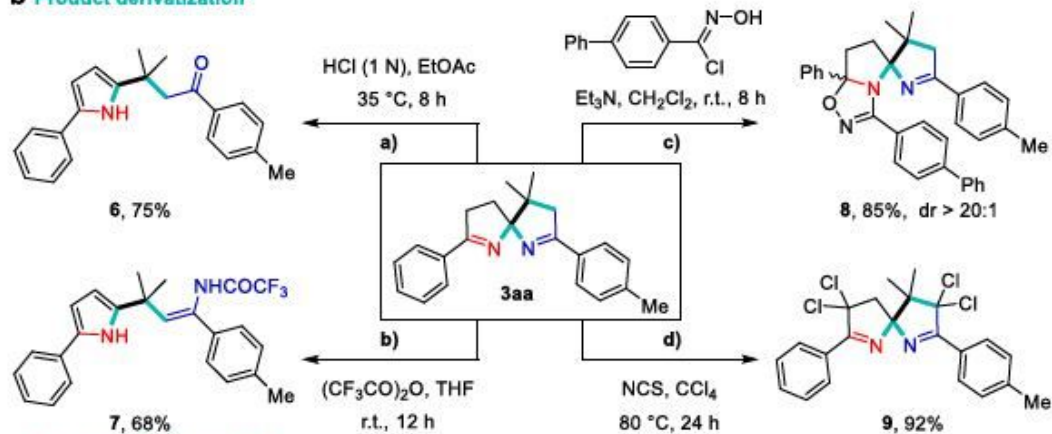
Figure 1

aReaction conditions: **4** (0.2 mmol), **2** (0.5 mmol), *fac*-Ir(ppy)₃ (2 mol %), K₂CO₃ (0.3 mmol), DMSO (2 mL), 30 W blue LEDs, argon atmosphere, r.t., 6 h, in a sealed tube; isolated yields based on **4** after the chromatographic purification.

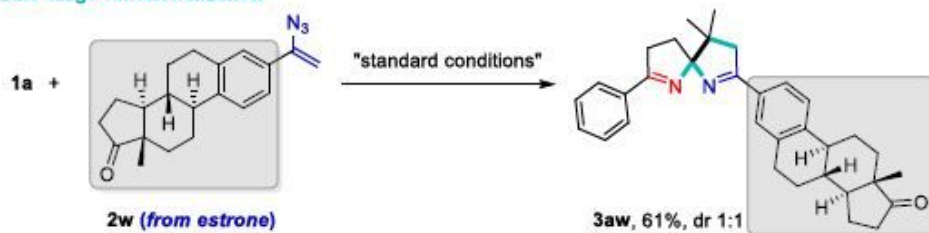
a Gram-scale reaction



b Product derivatization



c Late-stage functionalization



d Exploration of other vinyl azides and olefinic oxime esters

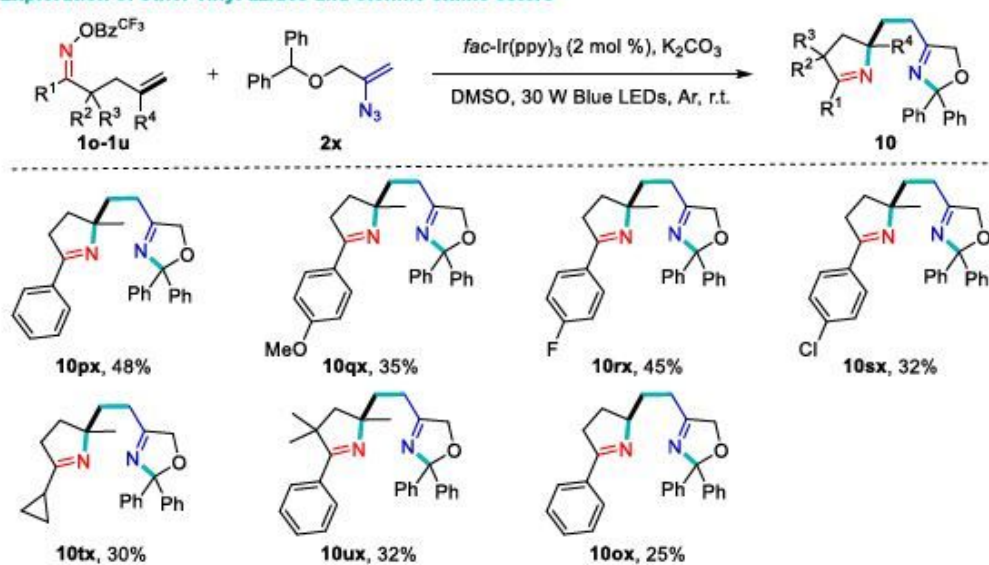
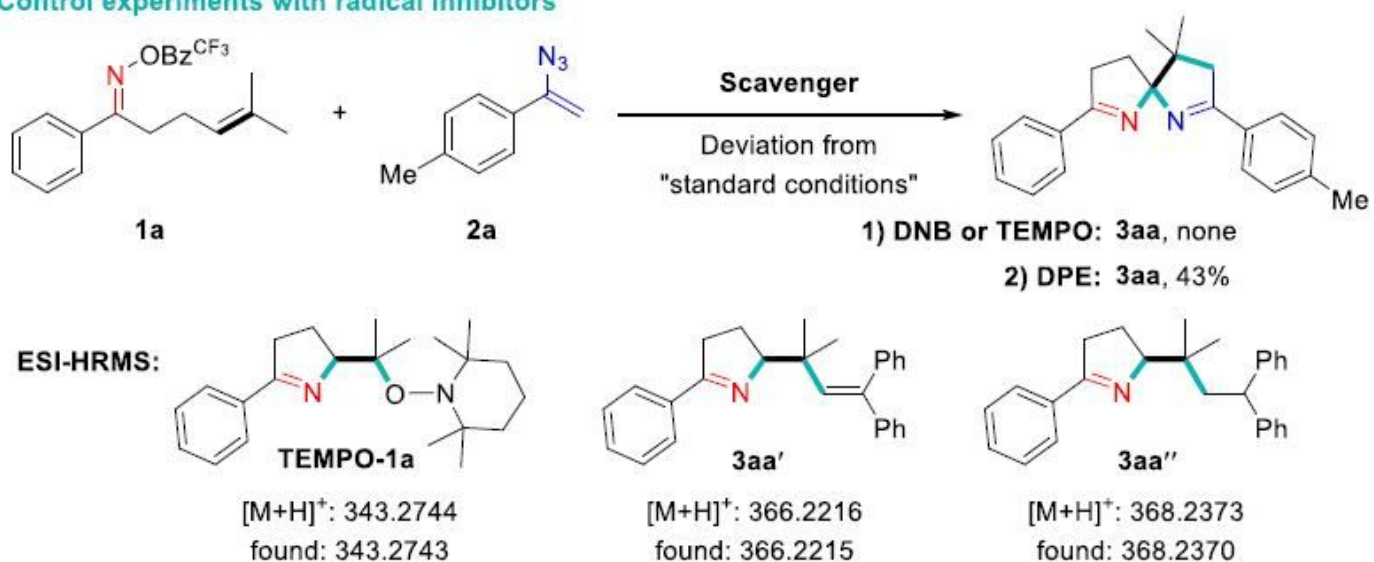


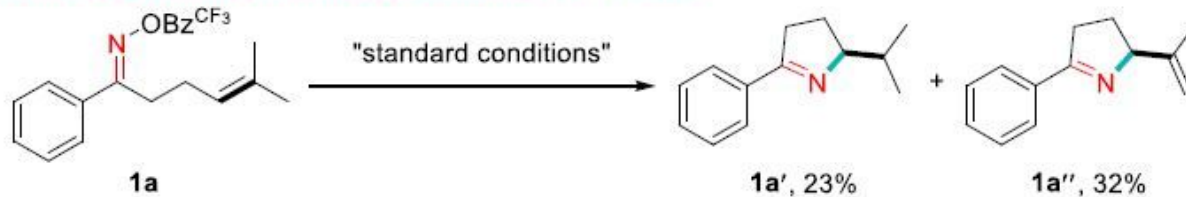
Figure 2

Gram-scale synthesis and synthetic applications of the reaction.

a Control experiments with radical inhibitors



b Control experiment without the addition of vinyl azide



c Control experiment using 2H-azirine instead of vinyl azide

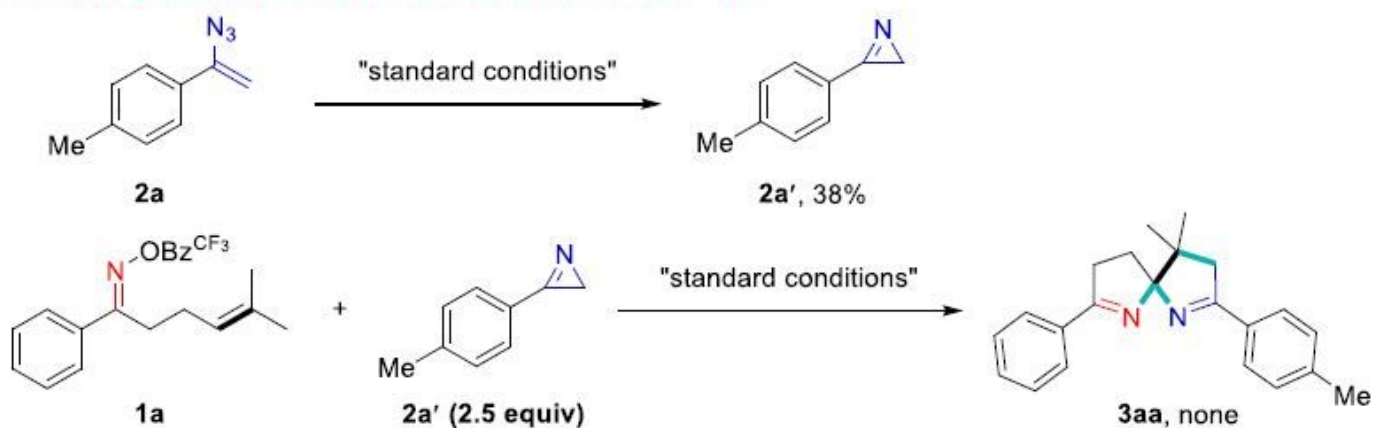
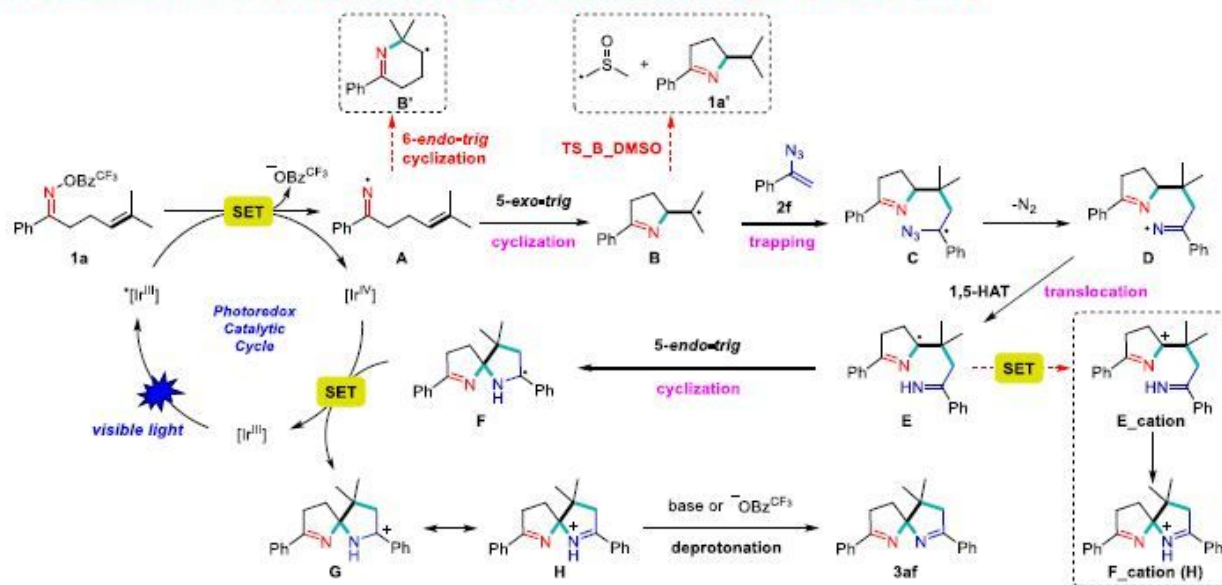


Figure 3

Preliminary mechanistic studies. a Control experiments with radical inhibitors. b Control experiment without the addition of vinyl azide. c Control experiment using 2H-azirine instead of vinyl azide.

a Proposed mechanism for the nitrogen radical-triggered trifunctionalizing ipso-spirocyclization



b Free energy profiles for the the nitrogen radical-triggered trifunctionalizing ipso-spirocyclization

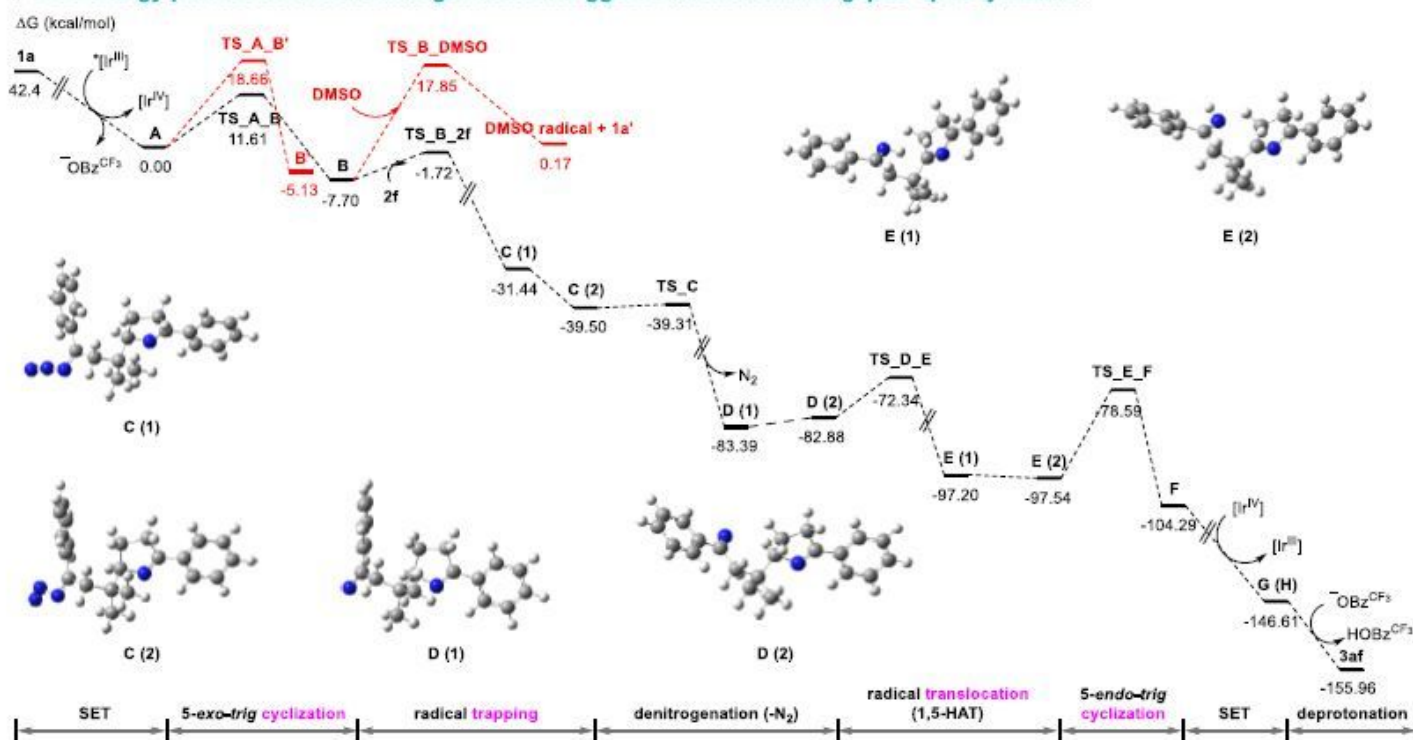


Figure 4

Proposed mechanism and free energy profiles for the nitrogen radical-triggered trifunctionalizing ipso-spirocyclization of unactivated alkenes. The values have been given in the unit of kcal mol⁻¹ and represent the relative free energies calculated using M06-2X method in DMSO solvent. Note: Two different energy values for one structure refer to conformer changes.

Supplementary Files

This is a list of supplementary files associated with this preprint. Click to download.

- [SIQZYNS.pdf](#)
- [SIQZYNS.pdf](#)